

Generic Misalignment Aberration Patterns in Wide-Field Telescopes

Paul L. Schechter

MIT Kavli Institute, Cambridge, MA 02139

schech@mit.edu

and

Rebecca Sobel Levinson

MIT Kavli Institute, Cambridge, MA 02139

rsobel@mit.edu

ABSTRACT

Axially symmetric telescopes produce well known “Seidel” off-axis third-order aberration patterns: coma, astigmatism, curvature of field and distortion. When axial symmetry is broken by the small misalignments of optical elements, additional third-order aberration patterns arise: one each for coma, astigmatism and curvature of field and two for distortion. Each of these misalignment patterns is characterized by an associated two-dimensional vector, each of which in turn is a linear combination of the tilt and decenter vectors of the individual optical elements. For an N -mirror telescope, $2(N - 1)$ patterns must be measured to keep the telescope aligned. For $N = 3$, as in a three mirror anastigmat, there is a two-dimensional “subspace of benign misalignment” over which the misalignment patterns for third-order coma, astigmatism and curvature of field are identically zero. One would need to measure at least one of the two distortion patterns to keep the telescope aligned. Alternatively, one might measure one of the fifth-order misalignment patterns, which are derived herein. But the fifth-order patterns are rather insensitive to misalignments, even with moderately wide fields, rendering them of relatively little use in telescope alignment. Another alternative would to use telescope pointing as part of the alignment solution.

Subject headings: telescopes – optics

1. Introduction

1.1. new telescopes, stringent constraints

The designs for several large telescopes that may get built in the next decade are driven largely by the need for superb and stable image quality over wide fields (Ma et al. 2008; Phillion et al. 2006). Perhaps the most demanding of the scientific programs that in turn drive these requirements is that of cosmological weak lensing, using galaxy images to measure gravitational shape distortions as small as as one part in ten thousand.

Of particular concern for ground-based telescopes are the rigid body motions of the optical elements due to gravitational and thermal stresses on the telescope structure.¹ The positions of the optical elements can be controlled only to the extent that they can be measured, putting a premium on the accurate characterization of the aberrations generated by telescope misalignments.

On the assumption that at least some of these aberrations are best measured with wavefront sensors, several questions immediately arise. How many aberrations must be measured? Which ones? At how many field positions must the measurements be made? Where?

One can always, as a last resort, attempt to answer these questions by simulation. But we argue here that the answers to these questions hinge on the identification of generic field aberration patterns that emerge in a wide variety of circumstances. A relatively small number of such patterns suffices to efficiently diagnose and correct misalignments. And only a small number of field points must be sampled to measure these patterns. Moreover two of the patterns may in some cases be determined directly from science data.

1.2. literature

The practical astronomical literature on the alignment of wide field telescopes is very limited. McLeod’s (1996) paper describing the use of coma and astigmatism patterns to align the Whipple Observatory 1.2-m telescope anchors the recent literature. Wilson & Delabre (1997) discuss the alignment of the ESO NTT. Gitton & Noethe (1998) describe the alignment of the ESO VLTs, and Noethe & Guisard (2000) give a more general description of the astigmatism patterns expected from two-mirror telescopes. Lee et al. (2008) give a general

¹Such telescopes are *also* subject to deformations of the optical elements, but on longer timescales than the rigid body motions.

treatment of third-order misalignment distortions and then discuss coma and astigmatism and curvature of field in their case studies. Palunas et al. (2010) describe the alignment of the Magellan Nasmyth telescopes using coma, astigmatism and curvature of field.

Maréchal (1950) derives the third-order misalignment aberration patterns for coma, astigmatism, curvature of field and distortion.

Thompson and collaborators (Shack & Thompson 1980; Thompson 2005; Thompson et al 2009) develop a formalism for analyzing telescope misalignments using a vector notation that is elegant and relatively transparent. It isolates generic misalignment patterns associated with third-order aberrations – coma, astigmatism, curvature of field and distortion – and beyond that, generic misalignment patterns associated with fifth-order aberrations.

In an unpublished M.S. thesis, Tessieres (2003) used ray tracing software to determine amplitudes for Thompson’s misalignment patterns, which at that time had only appeared in Thompson’s Ph.D. thesis (1980). Hvisc & Burge (2008) build on Tessieres’ work in modeling a four mirror corrector for the Hobby-Eberly Telescope. They identify the linear combinations of orthogonal aberration patterns (integrated over the field) that are most sensitive to the tilts and decenters of the mirrors.

1.3. outline

In the following sections we rederive these same misalignment aberration patterns, using the Thompson et al. vector notation but following instead the development of Schroeder (1987). The present paper is quite similar in spirit to Tessieres’: identify those aberration patterns of potential interest and ascertain which are of greatest value in aligning a telescope. However our approach differs in that, in the interest of efficiency, we ignore patterns that are non-linear in the tilts and decenters of the mirrors. This simplification is appropriate for small misalignments of an otherwise rotationally symmetric telescope. We also give somewhat greater consideration to the role of distortion, curvature of field and spherical aberration than did Tessieres.

In §2 we discuss the misalignment patterns produced by two-mirror telescopes, proceeding from the better known generic coma and astigmatism misalignment patterns, through the almost trivial curvature of field misalignment pattern, to the two distortion misalignment patterns. We then retrace our steps using a more general approach that shows how the misalignment patterns produced by an optic derive from the surface of that optic. In §3 we discuss the alignment of three-mirror telescopes. We note that distortion patterns, which might in principal be used for alignment, cannot be measured with conventional wavefront

sensors. In §4 we use the same methods used in §2 to deduce the misalignment patterns associated with fifth-order aberrations. In the course of this we attempt to systematize the somewhat ragged nomenclature associated with the fifth-order aberrations. We discuss the work of Tessieres (2003), which casts some doubt on the practical utility of fifth-order aberration patterns. In §5 we address a variety of complicating factors: mirror deformations, transmitting correctors, central obscurations and focal plane tilts. In §6 we discuss several ways in which the misalignment aberration patterns might be used, and why one might ultimately choose to forego their use.

2. Generic patterns and two-mirror telescopes

2.1. coma

McLeod’s (1996) paper shows how an astigmatic misalignment pattern can be used in conjunction with coma to align a telescope. McLeod’s first step is to center the secondary so as to zero the coma. He does not explicitly refer to a coma “pattern,” but it is widely appreciated that decentering the secondary of a Ritchey-Chretien telescope produces coma that is to first order constant across the field. For the present purposes we take this to be a pattern, albeit a boring one. McLeod does identify an astigmatism pattern, which he then renders symmetric by rotating the secondary about its coma-free pivot.

Schroeder (1987) calculates the the coma patterns that arise in a two mirror telescope, allowing for tilting and decentering the secondary. The comatic wavefront G^{coma} is a function of position on the pupil $\vec{\rho}$, with polar coordinates ρ and ϕ , and field angle $\vec{\sigma}$, with polar coordinates σ and θ :

$$G^{coma} = G_{Seidel}^{coma} \sigma \rho^3 \cos(\phi - \theta) + G_{decenter}^{coma} \ell \rho^3 \cos(\phi - \phi_\ell) + G_{tilt}^{coma} \alpha \rho^3 \cos(\phi - \phi_\alpha) \quad (1)$$

where $\vec{\ell}$ is the decenter of the secondary which projects to angle ϕ_ℓ on the pupil, and $\vec{\alpha}$ is the vector tilt of the secondary which projects to angle ϕ_α on the pupil. The first term on the right hand side gives the symmetric “Seidel” coma typical of an aligned two mirror telescope. The next two terms give the constant coma pattern typical of a decentering or tilt of the secondary. The coefficients G_{Seidel}^{coma} , $G_{decenter}^{coma}$, and G_{tilt}^{coma} depend upon the radii of curvature, R_i , and conic constants, K_i , of the two mirrors, the positions, s_i , and magnifications, m_i of the object for each mirror, and the distance from the primary mirror to the secondary, W . In a Ritchey-Chretien telescope the G^{coma} term is identically zero, giving no coma when aligned.

The notation here is different from that of Schroeder; the conversion from Schroeder’s to the present notation is given in appendix A.

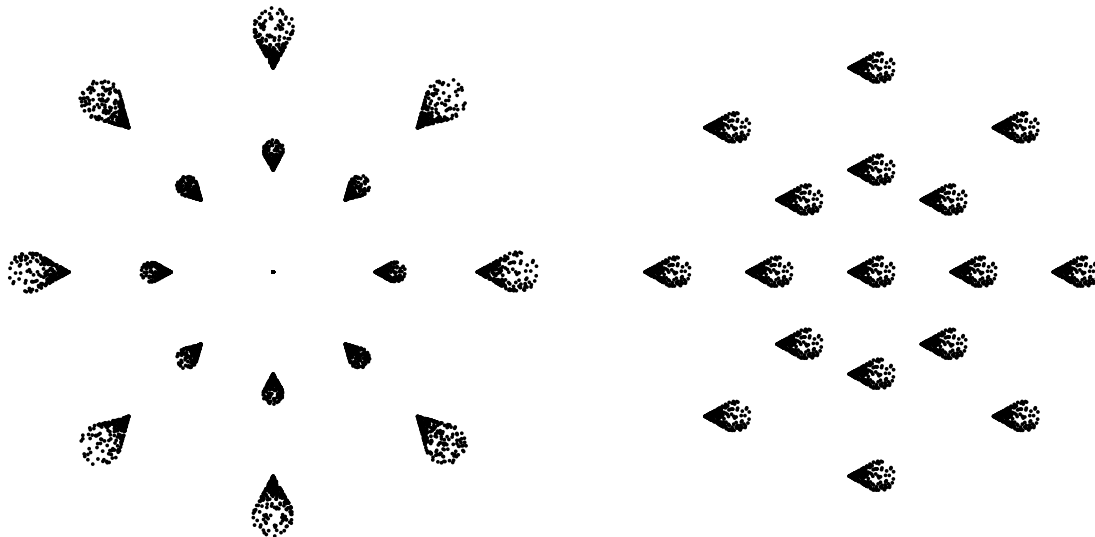


Fig. 1.— Comatic field patterns. (a) Seidel coma field pattern typical of an aligned telescope. (b) Constant coma indicating a tilt and (or) decentering of the secondary along the x axis.

The Seidel term varies linearly as field angle σ and as $\rho^3 \cos \phi$ and (or) $\rho^3 \sin \phi$ on the pupil. The tilt and decenter terms are constant over the field, but have the same functional dependence on pupil coordinates as the first term. We shall somewhat loosely refer to any aberration that has the same dependence upon pupil coordinates as “coma,” even when it does not have the Seidel coma dependence on field angle σ . Figure 1a shows the point spread function at various points in the field for the first term in equation (1). Figure 1b shows the point spread function pattern typical of either of the last two terms in equation (1).

2.2. astigmatism

Following Schroeder’s (1987) example for coma, McLeod (1996) calculated the corresponding astigmatism pattern for the case of a nulled field constant coma pattern. He finds an astigmatic wavefront, G^{astig} , given by:

$$G^{astig} = G_{sym}^{astig} \sigma^2 \rho^2 \cos 2(\phi - \theta) + G_{decenter}^{astig} \sigma \ell \rho^2 \cos(2\phi - \theta - \phi_\ell) + G_{tilt}^{astig} \sigma \alpha \rho^2 \cos(2\phi - \theta - \phi_\alpha) \quad (2)$$

The first term on the right gives the symmetric astigmatism typical of an aligned two mirror telescope. The next two terms give the astigmatism pattern typical of a decentering or tilt the secondary. The coefficients G_{sym}^{astig} , $G_{decenter}^{astig}$ and G_{tilt}^{astig} again depend upon the radii of curvature, R_i and conic constants, K_i of the two mirrors, the positions, s_i and magnifications, m_i of the object for each mirror, and the distance from the primary mirror to the secondary, W . The details of the conversion from McLeod’s notation to the above are given in appendix B.

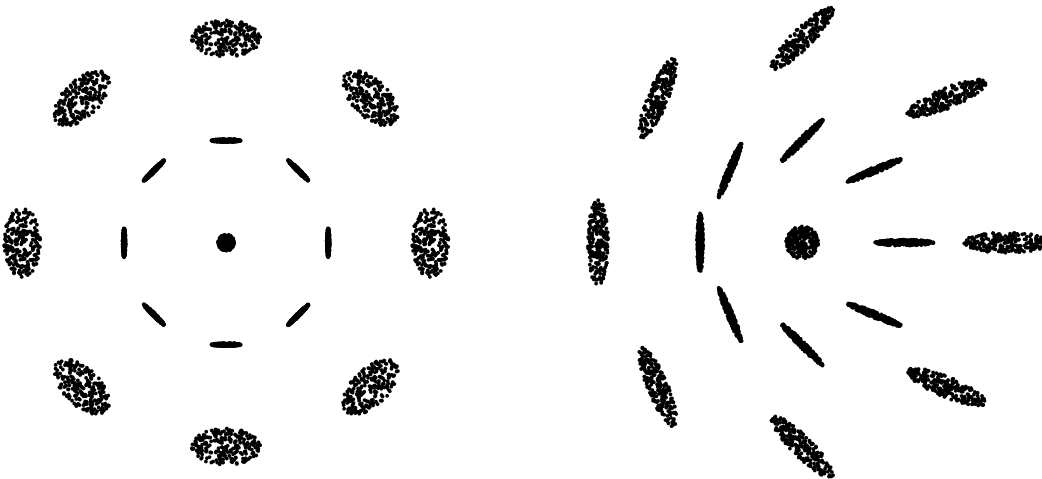


Fig. 2.— Astigmatic field patterns. (a) Symmetric astigmatism field pattern typical of an aligned telescope. A constant defocus has been added to show the orientation of the astigmatism. (b) Astigmatic field pattern indicating a tilt and (or) decentering of the secondary along the x axis.

The symmetric term varies as the square of the field radius σ and varies as $\rho^2 \cos 2\phi$ and (or) $\rho^2 \sin 2\phi$ on the pupil. This is almost, but not quite the variation associated with third-order, Seidel astigmatism.² It is readily decomposed into terms that vary as $\rho^2 \cos^2 \phi$ (Seidel astigmatism) and $\rho^2 \cos^0 \phi$ (Seidel curvature of field). The tilt and decenter terms have the same functional dependence on pupil coordinates as the symmetric term, but vary linearly with distance from the center of the field σ , and vary as the cosine and (or) sine of the field angle θ . We shall again refer loosely to any aberration that has the same dependence

²By convention “Seidel” astigmatism is taken to vary as $\rho^2 \cos^2 \phi$ on the pupil. By contrast “Zernike” astigmatism is almost always taken to vary as $\rho^2 \cos 2\phi$. The Seidel definition emerges naturally from the derivation of aberration patterns. The Zernike definition makes for more symmetric wavefronts and orthogonality among the different aberrations. A similar ambiguity arises in the definition of trefoil.

upon pupil coordinates as astigmatism, even when it does not have the Seidel dependence on field position. Figure 2a shows the point spread function at various points in the field for the symmetric term in equation (2). Figure 2b shows the point spread function pattern characteristic of either of the tilt or decenter terms in equation (2).

McLeod (1996) describes a single astigmatism pattern, which he symmetrizes in the course of aligning his telescope. Here we decompose this into two patterns, a symmetric one characteristic of an aligned telescope and an asymmetric one characteristic of a misaligned telescope.³

Both for coma and for astigmatism (and in the cases of the additional aberrations considered below) the misalignment pattern varies as one power of field radius less rapidly than the corresponding symmetric pattern.

2.3. curvature of field

Coma and astigmatism are just two of the five third-order Seidel aberrations. Curvature of field (henceforth COF) manifests itself as a defocus which varies as the square of the distance from the center of an assumed flat focal plane. McLeod might in principal have used curvature of field (rather than astigmatism) to align the Whipple 1.2-m, but there is a potential degeneracy with a tilted instrument. Following Schroeder and McLeod, we find an associated wavefront,

$$G^{COF} = G_{Seidel}^{COF} \sigma^2 \rho^2 + G_{decenter}^{COF} \sigma \ell \rho^2 \cos(\theta - \phi_\ell) + G_{tilt}^{COF} \sigma \alpha \rho^2 \cos(\theta - \phi_\alpha). \quad (3)$$

The first term on the right hand side gives the symmetric Seidel curvature of field typical of an aligned two mirror telescope, and the next two give the defocus patterns typical of a decenter or tilt of the secondary. The coefficients G_{Seidel}^{COF} , $G_{decenter}^{COF}$, and G_{tilt}^{COF} again depend upon the radii of curvature, R_i and conic constants, K_i of the two mirrors, the positions, s_i and magnifications, m_i of the object for each mirror, and the distance from the primary mirror to the secondary, W . The details of the derivation of the above are given in appendix

³The “dreamcatcher” plot of Figure 2b makes cameo appearances in a number of contexts. It can be seen in a map of image elongations at the prime focus of the LBT (Romano et al. 2010) and in the point spread function map, Figure 4.14, in version 12.0 of the Chandra Proposer’s Observatory Guide (Chandra X-ray Center 2009). The first such plot of which the authors are aware is in the paper by Shack & Thompson (1980). Maréchal (1950) comes close plotting the magnitude and orientation of the misalignment astigmatism pattern but suppressing the sign.

C.

The Seidel term varies as the square of the field radius σ and varies as ρ^2 on the pupil. But the dependence on pupil position is exactly the same as that of defocus, which is a first-order aberration. Anticipating the nomenclature introduced in §4 below, curvature of field might equally well be called “third-order defocus,” but we bow to convention. The tilt and decenter terms vary linearly with distance from a line passing through the center of the field, but have the same functional dependence on pupil coordinates. This is precisely what one would expect for a tilted focal plane. Figure 3a shows the point spread function at various points in the field for the Seidel term in equation (3). Figure 3b shows the point spread function pattern typical of either the tilt or decenter terms in equation (3).

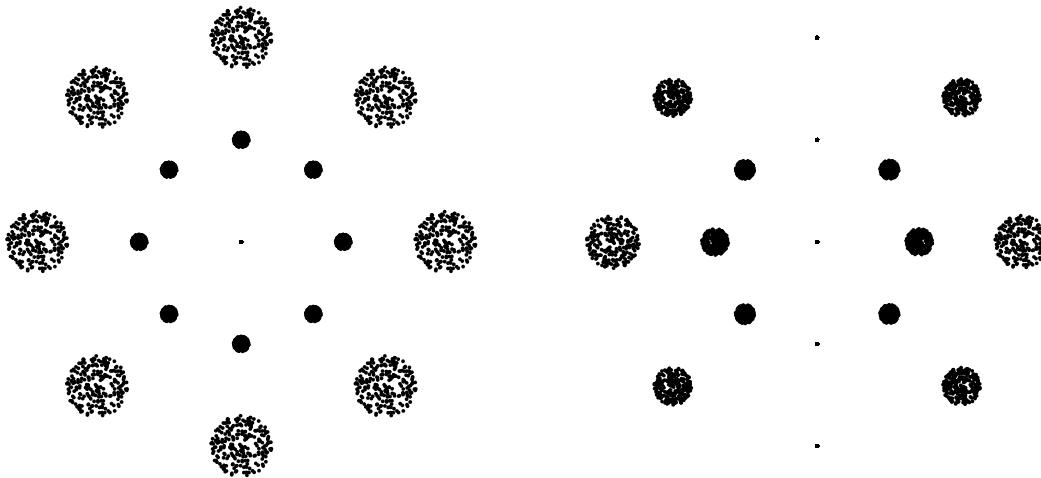


Fig. 3.— Curvature of field patterns. (a) Seidel COF typical of an aligned telescope. (b) COF field indicating a tilt and (or) decenter of the secondary along the x axis.

2.4. distortion

While distortion is one of the five Seidel aberrations, for many purposes it can be neglected, since it does not degrade image quality. Distortion does, however alter the positions of images in the field, and of particular interest for the measurements of weak gravitational lensing, it changes the shapes of extended objects. And most importantly for the present discussion it may be of some use in aligning a telescope.

Following the conventions of Schroeder and McLeod, we find the associated wavefront

delay for a misaligned two mirror telescope:

$$\begin{aligned}
 G^{distortion} &= G_{Seidel}^{distortion} \sigma^3 \rho \cos(\phi - \theta) \\
 &+ G_{decenter,\sigma}^{distortion} \sigma^2 \ell \cos(\theta - \phi_\ell) \rho \cos(\phi - \theta) + G_{decenter,\rho}^{distortion} \sigma^2 \ell \rho \cos(\phi - \phi_\ell) \\
 &+ G_{tilt,\sigma}^{distortion} \sigma^2 \alpha \cos(\theta - \phi_\alpha) \rho \cos(\phi - \theta) + G_{tilt,\rho}^{distortion} \sigma^2 \alpha \rho \cos(\phi - \phi_\alpha)
 \end{aligned} \tag{4}$$

The Seidel term on the right varies as the cube of field angle σ and as $\rho \cos \phi$ and (or) $\rho \sin \phi$ on the pupil. Distortion differs from coma, astigmatism and curvature of field in having two distinct misalignment aberration patterns rather than only one. We will encounter several similar pairs of misalignment aberration patterns when we consider fifth-order misalignment patterns in §4. The two terms are distinguished by whether the direction of the tilt, $\vec{\alpha}$ or decenter, $\vec{\ell}$ enters in a dot product with the field position, $\vec{\sigma}$ or the pupil position, $\vec{\rho}$. We use “ σ ” and “ ρ ” to label the two alternatives.

The σ terms have the same functional dependence on pupil coordinates as the Seidel term, but are proportional to the square field angle σ and the cosine of its polar coordinate, θ . These produce a field distortion pattern directed radially outward, but with a magnitude that depends on the product of the field angle and its projection onto the decenter or tilt.

The ρ terms also have the same functional dependence on pupil coordinates as the first, but vary only as the square field angle σ . The direction of the distortion is that of the decenter or tilt, but its magnitude increases outward as the square of the distance from the center of the field.

The three distortion patterns are shown in figure 4. Details of the derivation of the coefficients are given in appendix D.

Each of the two distinct misalignment distortion patterns is characterized by a two-vector. Were one able to measure those vectors with the same accuracy as the two-vectors that characterize coma and astigmatism one might in principle use *only* distortion measurements to align a two mirror telescope.

2.5. spherical aberration

Spherical aberration is the fifth of the Seidel aberrations and is constant across the field. Tilts and decenters do not produce asymmetric spherical aberration patterns.

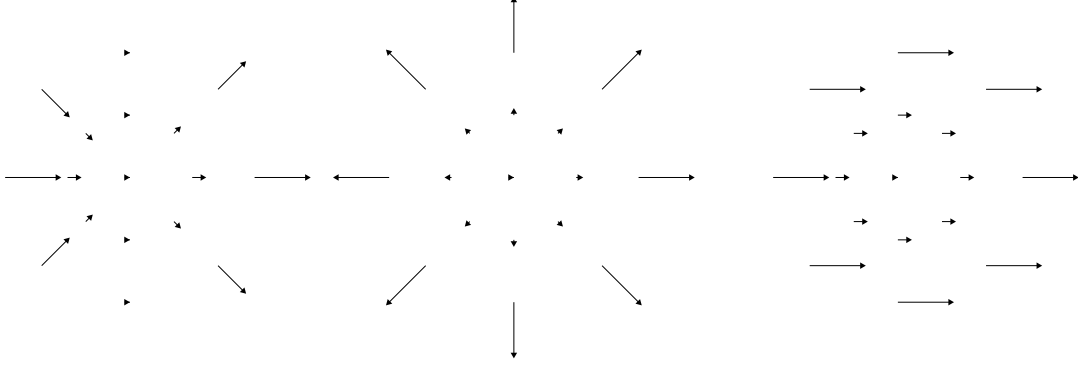


Fig. 4.— Distortion field patterns. (a) The “ σ ” distortion pattern indicating a tilt and (or) decentering of the secondary along the x axis. (b) Seidel distortion typical of an aligned telescope. (c) The “ ρ ” distortion pattern indicating a tilt and (or) decentering of the secondary along the x axis.

2.6. generalization

In the preceding subsections the third-order aberrations were cast so as to display explicitly the azimuthal dependence upon pupil position, $\vec{\rho}$ and field angle, $\vec{\sigma}$. These can be recast more compactly and transparently in vector form. For example the Seidel distortion terms above varies as $(\vec{\sigma} \cdot \vec{\sigma})(\vec{\sigma} \cdot \vec{\rho})$.

Suppose a single mirror i serves as its own pupil. The wavefront delay G^{3rd} for a ray that intercepts the mirror at position $\vec{\omega}$ and that makes an angle $\vec{\psi}$ with the axis of the mirror is given by⁴

$$\begin{aligned}
 G^{3rd} = & W_{040} \left(\frac{\vec{\omega}}{R} \cdot \frac{\vec{\omega}}{R} \right) \left(\frac{\vec{\omega}}{R} \cdot \frac{\vec{\omega}}{R} \right) + W_{131} \left(\vec{\psi} \cdot \frac{\vec{\omega}}{R} \right) \left(\frac{\vec{\omega}}{R} \cdot \frac{\vec{\omega}}{R} \right) \\
 & + W_{222} \left(\vec{\psi} \cdot \frac{\vec{\omega}}{R} \right) \left(\vec{\psi} \cdot \frac{\vec{\omega}}{R} \right) + W_{220} \left(\vec{\psi} \cdot \vec{\psi} \right) \left(\frac{\vec{\omega}}{R} \cdot \frac{\vec{\omega}}{R} \right) \\
 & + W_{311} \left(\vec{\psi} \cdot \vec{\psi} \right) \left(\vec{\psi} \cdot \frac{\vec{\omega}}{R} \right)
 \end{aligned} \tag{5}$$

where W_{040} is the spherical aberration coefficient, W_{131} is the coma coefficient, W_{222} is the astigmatism coefficient, W_{220} is the curvature of field coefficient, and W_{311} is the distortion

⁴We reserve $\vec{\rho}$ for the position on the pupil when the optic is despaced from the pupil.

coefficient. These aberration coefficients depend only on the curvature of the mirror, R , the conic constant of the mirror, K , the magnification of the mirror, m , and the position of the object for the mirror, s . Schroeder (1987) in §§5.1 of his book shows that the aberrations which vary linearly with ray height on the optic must be zero for conic section optics which serve as their own pupils. We therefore set W_{311} to zero and ignore it in the following discussion.

Following Schroeder (1987), one finds that if the pupil is offset by W along the axis of the mirror, the position at which a ray lands on the mirror, $\vec{\omega}$ depends upon its position on the pupil, $\vec{\rho}$ and the angle the chief ray makes to the pupil normal, $\vec{\sigma}$ (which is defined to be the field angle), and upon W . The angle that the ray makes with the axis of the mirror, $\vec{\psi}$ depends upon field angle $\vec{\sigma}$ and the pupil offset, W .

If the mirror is tilted by angle $\vec{\alpha}$, it changes the angle $\vec{\psi}$ that a ray makes with the mirror's axis. And if the mirror is decentered from the optical axis (which is perpendicular to and centered on the pupil) by \vec{l} , it changes both the position at which a ray lands on the mirror, $\vec{\omega}$ and the angle $\vec{\psi}$ that the ray makes with respect to the mirror's axis.

The net effect of a pupil offset or a misalignment of the mirror relative to the pupil is to shift the position $\vec{\omega}$ at which a given ray strikes the mirror and to change the angle $\vec{\psi}$ that the ray makes with the axis of the mirror. The transformations from pupil coordinates, $\vec{\rho}$ and field angle, $\vec{\sigma}$ to mirror coordinates and mirror angle for a mirror despaced by an amount W and decentered and tilted by \vec{l} and $\vec{\alpha}$ are then

$$\vec{\psi} = \left(1 - \frac{W}{s}\right)\vec{\sigma} - \left(\vec{\alpha} + \frac{\vec{l}}{s}\right) \quad (6)$$

$$\vec{\omega} = (\vec{\rho} - W\vec{\psi}) - \vec{l}. \quad (7)$$

An offset of the pupil from the mirror by an amount W causes what was Seidel spherical aberration to manifest itself as a combination of spherical aberration, coma, astigmatism, curvature of field and distortion, all of which have the symmetric Seidel field dependence. Likewise what was coma manifests itself as a combination of coma, astigmatism, curvature of field and distortion. This cascade downward from spherical to coma to astigmatism and curvature of field and finally to distortion is embodied in the “stop shift” formulae (e.g. Wilson 1996).

Decenterings and tilts of the mirror relative to the pupil also produce cascades. For an axially symmetric telescope we may assume that these tilts and decenters are small and ignore terms that are quadratic and higher in either or both. In the aberration patterns

associated with the surviving linear terms, a field angle vector $\vec{\sigma}$ is replaced by either a tilt, $\vec{\alpha}$ or a decenter, $\vec{\ell}/R$. The field angle exponents for the misalignment aberration patterns are therefore smaller by one than those of the corresponding Seidel aberrations.

Table 1 gives aberration patterns that arise when an optic is offset by W with respect to its pupil, and decentered and tilted by small amounts.

The different signs for odd and even numbered mirrors arise from the fact that the chief ray for a given optic may be traveling in the opposite direction than the chief ray on the pupil for the primary mirror, which here determines the field angle $\vec{\sigma}$. The σ -type distortion patterns have factors $\vec{\sigma} \cdot \frac{\vec{l}}{R}$ or $\vec{\sigma} \cdot \vec{\alpha}$. The ρ -type distortion patterns have factors $\vec{\rho} \cdot \frac{\vec{l}}{R}$ or $\vec{\rho} \cdot \vec{\alpha}$.

2.7. application to 2-mirror telescopes and 2.5-mirror telescopes

Table 1 of the previous subsection gives the third-order aberrations for a single mirror with a pupil offset by W along the optical axis. The aberrations for a 2-mirror telescope are found by computing the elements of two such tables, one for the primary and one for the secondary, and adding.

For many two-mirror telescopes the pupil is coincident with the primary. If one also takes the primary to define the pointing of the telescope, one can take the pupil offset, W_1 , the mirror decenter, $\vec{\ell}_1$ and the mirror tilt, $\vec{\alpha}_1$ all to be zero. The misalignment patterns are then due entirely to the decenter, $\vec{\ell}_2$ and tilt, $\vec{\alpha}_2$ of the secondary. One need only measure two of the five misalignment patterns in Table 1 to align a telescope. McLeod (1996) measures coma and astigmatism. He might in principle have used the two distortion patterns, but these would require a high precision astrometric catalog (perhaps using galaxy positions to avoid the effects of stellar proper motions). Moreover as the misalignment distortion patterns vary as a higher powers of field angle than the misalignment astigmatism and coma patterns, they might be expected to have smaller amplitudes. McLeod might also have used curvature of field, although here there is the danger that the detector might be tilted with respect to the primary. Or, had he been feeling particularly masochistic, he might have measured all five patterns, for the sake of redundancy.

With their folding flats, the Magellan telescopes in their Nasmyth configuration qualify as 2.5-mirror telescopes. One need not worry about the decentering of the tertiary but one must measure and correct for its tilt, $\vec{\alpha}_3$. The alignment procedure described by Palunas et al. (2010) adds the curvature of field misalignment pattern (equivalent to a focal plane tilt) to those of coma and astigmatism.

Table 1. Symmetric and asymmetric aberration patterns for mirrors offset, decentered and tilted with respect to the pupil.

aberration	pupil offset W	decenter $\vec{\ell}$	tilt $\vec{\alpha}$
spherical	$(\frac{\vec{\rho}}{R} \cdot \frac{\vec{\rho}}{R})(\frac{\vec{\rho}}{R} \cdot \frac{\vec{\rho}}{R}) \times W_{040}$		
coma	$(\frac{\vec{\rho}}{R} \cdot \frac{\vec{\rho}}{R})(\frac{\vec{\rho}}{R} \cdot \vec{\sigma}) \times \mp^a [$ $(\frac{W}{s} - 1) W_{131}$ $+ 4\frac{W}{R} W_{040}]$	$(\frac{\vec{\rho}}{R} \cdot \frac{\vec{\rho}}{R})(\frac{\vec{\rho}}{R} \cdot \frac{\vec{\ell}}{R}) \times [$ $-\left(\frac{R}{s}\right) W_{131}$ $- 4W_{040}]$	$(\frac{\vec{\rho}}{R} \cdot \frac{\vec{\rho}}{R})(\frac{\vec{\rho}}{R} \cdot \vec{\alpha}) \times [$ $-W_{131}]$
astigmatism	$(\frac{\vec{\rho}}{R} \cdot \vec{\sigma})(\frac{\vec{\rho}}{R} \cdot \vec{\sigma}) \times [$ $(\frac{W}{s} - 1)^2 W_{222}$ $+ 2\frac{W}{R} (\frac{W}{s} - 1) W_{131}$ $+ 4\frac{W^2}{R^2} W_{040}]$	$(\frac{\vec{\rho}}{R} \cdot \vec{\sigma})(\frac{\vec{\rho}}{R} \cdot \frac{\vec{\ell}}{R}) \times \pm^a [$ $2\left(\frac{R}{s}\right) (\frac{W}{s} - 1) W_{222}$ $+ 2\left(\frac{2W}{s} - 1\right) W_{131}$ $+ 8\frac{W}{R} W_{040}]$	$(\frac{\vec{\rho}}{R} \cdot \vec{\sigma})(\frac{\vec{\rho}}{R} \cdot \vec{\alpha}) \times \pm^a [$ $2\left(\frac{W}{s} - 1\right) W_{222}$ $+ 2\frac{W}{R} W_{131}]$
COF	$(\frac{\vec{\rho}}{R} \cdot \frac{\vec{\rho}}{R})(\vec{\sigma} \cdot \vec{\sigma}) \times [$ $\frac{1}{2} (\frac{W}{s} - 1)^2 W_{220}$ $+ \frac{W}{R} (\frac{W}{s} - 1) W_{131}$ $+ 2\frac{W^2}{R^2} W_{040}]$	$(\frac{\vec{\rho}}{R} \cdot \frac{\vec{\rho}}{R})(\vec{\sigma} \cdot \frac{\vec{\ell}}{R}) \times \pm^a [$ $2\left(\frac{R}{s}\right) (\frac{W}{s} - 1) W_{220}$ $+ \left(\frac{2W}{s} - 1\right) W_{131}$ $+ 4\frac{W}{R} W_{040}]$	$(\frac{\vec{\rho}}{R} \cdot \frac{\vec{\rho}}{R})(\vec{\sigma} \cdot \vec{\alpha}) \times \pm^a [$ $2\left(\frac{W}{s} - 1\right) W_{220}$ $+ \frac{W}{R} W_{131}]$
distortion	$(\frac{\vec{\rho}}{R} \cdot \vec{\sigma})(\vec{\sigma} \cdot \vec{\sigma}) \times \mp^a [^b$ $2\frac{W}{R} (\frac{W}{s} - 1)^2 W_{220}$ $+ 2\frac{W}{R} (\frac{W}{s} - 1)^2 W_{222}$ $+ 3\frac{W^2}{R^2} (\frac{W}{s} - 1) W_{131}$ $+ 4\frac{W^3}{R^3} W_{040}]$	$(\frac{\vec{\rho}}{R} \cdot \frac{\vec{\ell}}{R})(\vec{\sigma} \cdot \vec{\sigma}) \times [$ $-2\left(\frac{W}{s} - 1\right)^2 W_{220}$ $- 2\left(\frac{W}{s}\right) (\frac{W}{s} - 1) W_{222}$ $- 2\frac{W}{R} \left(\frac{3W}{2s} - 1\right) W_{131}$ $- 4\frac{W^2}{R^2} W_{040}]$ $(\frac{\vec{\rho}}{R} \cdot \vec{\sigma})(\vec{\sigma} \cdot \frac{\vec{\ell}}{R}) \times [$ $- 4\left(\frac{W}{s}\right) (\frac{W}{s} - 1) W_{220}$ $- 2\left(\frac{W}{s} - 1\right) \left(\frac{2W}{s} - 1\right) W_{222}$ $- 4\frac{W}{R} \left(\frac{3W}{2s} - 1\right) W_{131}$ $- 8\frac{W^2}{R^2} W_{040}]$	$(\frac{\vec{\rho}}{R} \cdot \vec{\alpha})(\vec{\sigma} \cdot \vec{\sigma}) \times [$ $- 2\frac{W}{R} (\frac{W}{s} - 1) W_{222}$ $- \frac{W^2}{R^2} W_{131}]$ $(\frac{\vec{\rho}}{R} \cdot \vec{\sigma})(\vec{\sigma} \cdot \vec{\alpha}) \times [$ $- 4\frac{W}{R} (\frac{W}{s} - 1) W_{220}$ $- 2\frac{W}{R} (\frac{W}{s} - 1) W_{222}$ $- 2\frac{W^2}{R^2} W_{131}]$

^aThe upper sign is for a primary, tertiary, or other odd numbered mirror. The lower sign is for a secondary or even numbered mirror.

^bThe W_{311} term has been omitted as it is equal to zero.

3. Aligning 3-mirror telescopes using distortion patterns

Calculating the aberration patterns for a 3-mirror telescope (say a three mirror anastigmat, henceforth a TMA) is not quite twice as difficult as for a 2-mirror telescope. One applies Table 1 to the tertiary and finds misalignment patterns that depend upon the decenter $\vec{\ell}_3$ and tilt $\vec{\alpha}_3$ of the tertiary. If the stop is coincident with the primary, only the secondary and tertiary both contribute to all five of the third-order misalignment patterns in Table 1. The patterns are linear in the decenter and tilt vectors, so that the combined wavefront gives the same five patterns, each characterized by a new pattern 2-vector. Each pattern 2-vector, $\vec{\mu}$, is a linear combination of the four misalignment 2-vectors, the tilts $\vec{\alpha}_2$ and $\vec{\alpha}_3$, and the decenters $\vec{\ell}_2$ and $\vec{\ell}_3$.

If coma, astigmatism and curvature of field are the only aberrations that adversely affect science, there is a two-dimensional “subspace of benign misalignment” for which the coma, astigmatism and curvature of field misalignment patterns are all zero in the limit of small misalignments. But if one does not bring additional information to bear, one runs the risk of drifting increasingly far from perfect alignment. This would produce large misalignment distortion, and ultimately, fifth-order misalignment patterns and third-order patterns that depend quadratically on the mirror tilts and decenters.

To measure the misalignment distortion patterns one would need pre-existing astrometry. The accuracy with which the distortion patterns could be measured would then be limited by the accuracy of the astrometric catalog. Moreover, as the misalignment distortion pattern varies as a higher power of field angle than the misalignment astigmatism and coma, it might be expected to have a smaller amplitude for a given tilt or decenter. This raises the question of whether one might use fifth-order aberration patterns to keep the telescope aligned.

4. Generic fifth-order aberration patterns

4.1. fifth-order aberrations for a single mirror

In §2.6 we considered the third-order aberrations produced by a single mirror with a stop at the mirror. The generalization to fifth-order is straightforward. The fifth-order wavefront delay, G^{5th} for a ray that hits the mirror at position \vec{c} and that makes an angle $\vec{\psi}$ with the axis of the mirror is given by

$$\begin{aligned}
 G^{5th} = & W_{060} \left(\frac{\vec{\omega}}{R} \cdot \frac{\vec{\omega}}{R} \right) \left(\frac{\vec{\omega}}{R} \cdot \frac{\vec{\omega}}{R} \right) \left(\frac{\vec{\omega}}{R} \cdot \frac{\vec{\omega}}{R} \right) + W_{151} \left(\frac{\vec{\omega}}{R} \cdot \frac{\vec{\omega}}{R} \right) \left(\frac{\vec{\omega}}{R} \cdot \frac{\vec{\omega}}{R} \right) \left(\frac{\vec{\omega}}{R} \cdot \vec{\psi} \right) \\
 & + W_{242} \left(\frac{\vec{\omega}}{R} \cdot \frac{\vec{\omega}}{R} \right) \left(\frac{\vec{\omega}}{R} \cdot \vec{\psi} \right) \left(\frac{\vec{\omega}}{R} \cdot \vec{\psi} \right) + W_{240} \left(\frac{\vec{\omega}}{R} \cdot \frac{\vec{\omega}}{R} \right) \left(\frac{\vec{\omega}}{R} \cdot \frac{\vec{\omega}}{R} \right) (\vec{\psi} \cdot \vec{\psi}) \\
 & + W_{333} \left(\frac{\vec{\omega}}{R} \cdot \vec{\psi} \right) \left(\frac{\vec{\omega}}{R} \cdot \vec{\psi} \right) \left(\frac{\vec{\omega}}{R} \cdot \vec{\psi} \right) + W_{331} \left(\frac{\vec{\omega}}{R} \cdot \frac{\vec{\omega}}{R} \right) \left(\frac{\vec{\omega}}{R} \cdot \vec{\psi} \right) (\vec{\psi} \cdot \vec{\psi}) \\
 & + W_{422} \left(\frac{\vec{\omega}}{R} \cdot \vec{\psi} \right) \left(\frac{\vec{\omega}}{R} \cdot \vec{\psi} \right) (\vec{\psi} \cdot \vec{\psi}) + W_{420} \left(\frac{\vec{\omega}}{R} \cdot \frac{\vec{\omega}}{R} \right) (\vec{\psi} \cdot \vec{\psi}) (\vec{\psi} \cdot \vec{\psi}) \\
 & + W_{511} \left(\frac{\vec{\omega}}{R} \cdot \vec{\psi} \right) (\vec{\psi} \cdot \vec{\psi}) (\vec{\psi} \cdot \vec{\psi})
 \end{aligned} \tag{8}$$

Since the pupil is coincident with the mirror, we might equally well have written the same equations but with position on the mirror $\vec{\omega}$ replaced by position on the pupil $\vec{\rho}$ and the angle that a ray makes with the axis of the mirror, $\vec{\psi}$ replaced by the field angle $\vec{\sigma}$. For the remainder of this subsection we shall take $\vec{\rho} = \vec{\omega}$ and $\vec{\sigma} = \vec{\psi}$.

4.1.1. W_{511} : fifth-order distortion

The W_{511} term has the same variation on the pupil as distortion, but varies as field angle to the fifth. We shall refer to this as “fifth-order distortion.”⁵

4.1.2. W_{420} : fifth-order defocus

The W_{420} term has the same variation on the pupil as defocus, and produces a point spread function indistinguishable from that of Seidel curvature of field. But as this term varies as the fourth power of field angle rather than quadratically, we call this term “fifth-order defocus.”

⁵Our nomenclature is driven primarily by the functional form of the aberration on the pupil. Thus an aberration that varies as $\rho^3 \cos \phi$ is referred to as coma. In this scheme third-order (Seidel) coma varies linearly with field angle and fifth-order coma varies as the cube of field angle. By contrast, the term that varies as $\rho^5 \cos \phi$ on the pupil is referred to here as second coma or coma-II. Hopkins (1950) calls this term fifth-order coma, but from our pupil oriented perspective this term, albeit one of fifth-order, cannot be called coma, which can only vary as $\rho^3 \cos \phi$. Curiously, we agree with Hopkins in calling the term that varies as $\rho^2 \cos^2 \phi$ fifth-order astigmatism and in calling the term that varies as $\rho \cos \phi$ fifth-order distortion. We reserve the term “Zernike” aberrations for the orthogonalized linear combinations of aberrations described here.

4.1.3. W_{422} : fifth-order astigmatism

The W_{422} term has the same variation on the pupil as third-order astigmatism, and produces a point spread function indistinguishable from it. But as this term varies as the fourth power of field angle rather than quadratically, we call this term “fifth-order astigmatism.” Again as with third-order astigmatism, this term varies on the pupil as $\rho^2 \cos^2 \phi$. It can be decomposed into a term that varies as Zernike astigmatism, $\rho^2 \cos 2\phi$, and a second that varies as defocus, $\rho^2 \cos^0 \phi$,

4.1.4. W_{311} : fifth-order coma

The W_{311} term has the same variation on the pupil as coma, but varies as field angle cubed. We call this “fifth-order coma.”

4.1.5. W_{333} : trefoil

The W_{333} term varies as $\rho^3 \cos^3 \phi$ on the pupil and as field angle cubed. None of the third-order aberrations has this behavior on the pupil; here we call it trefoil. This term can be decomposed into a term that varies as Zernike trefoil, $\rho^3 \cos 3\phi$, and a second that varies as coma, $\rho^3 \cos \phi$. Figure 5 shows the point spread function due to Zernike trefoil with varying amounts of an aberration that varies as ρ^3 added to it.

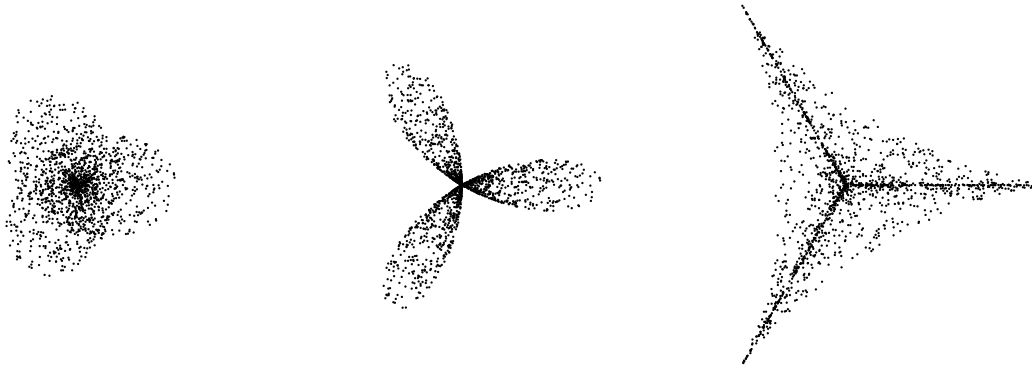


Fig. 5.— Point spread functions due to trefoil with $G^{tref} = \rho^3 \cos 3\phi$. Increasing amounts of a symmetric wavefront $G^{sym} = \rho^3$ have been added to bring out the three-fold symmetry of the wavefront. (a) $+\frac{2}{5}G^{sym}$ (b) $+G^{sym}$ (c) $+2G^{sym}$

4.1.6. W_{240} : *fifth-order spherical*

The W_{240} has the same variation on the pupil as spherical aberration, but varies as field angle squared. We shall refer to this as this “fifth-order spherical.”

4.1.7. W_{242} : *second astigmatism*

The W_{242} term varies as $\rho^4 \cos^2 \phi$ on the pupil. The angular dependence is that of astigmatism but the radial dependence is quartic not quadratic. We shall call this “second astigmatism” or “astigmatism-II.” Figure 6 shows the PSFs for second astigmatism with increasing amounts of spherical aberration added.



Fig. 6.— Point spread functions due to second astigmatism with $G^{astig-II} = \rho^4 \cos 2\phi$. In the second, third, and fourth cases increasing amounts of a spherical aberration $G^{sph} = \rho^4$ have been added. (a) pure second astigmatism (b) $+\frac{1}{2}G^{sph}$ (c) $+G^{sph}$ (d) $+\frac{3}{2}G^{sph}$

4.1.8. W_{151} : *second coma*

The W_{151} term varies as $\rho^5 \cos \phi$ on the pupil. The azimuthal dependence is that of coma but the radial dependence is quintic not cubic. We shall refer to this as “second coma” or “coma-II.” Figure 7 shows a PSF produced by second coma alongside one produced by ordinary (first) coma.

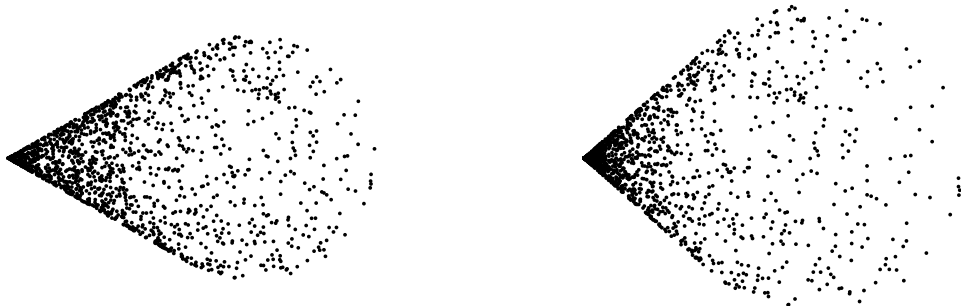


Fig. 7.— (a) Off axis (ordinary) coma PSF for the third-order and fifth-order coma patterns. The sine of the apex half angle is $1/2$, giving an apex angle of 60° . (b) Off axis second coma PSF. The sine of the apex half angle is $2/3$, giving an apex angle of 83.6° .

4.1.9. W_{060} : second spherical

We shall call the W_{060} “second spherical” or “spherical-II.” Were we strictly consistent we would have called spherical aberration “second defocus” and would have called this “third defocus” but as Emerson says, a foolish consistency is the hobgoblin of a small mind.

4.2. fifth-order aberrations for misaligned systems

Tilts and decenterings of mirrors produce misalignment patterns in a manner entirely analogous to those of third-order aberrations. The dependence upon field and pupil position and the first order dependence on misalignments are given in Table 2. Equations (6) and (7) are used to transform from the positions and angles with respect to the optic, $\vec{\omega}$ and $\vec{\psi}$ of equation (8) to positions and angles with respect the pupil, $\vec{\rho}$ and $\vec{\sigma}$. Terms with the same dependence on both of the latter are then added. The vectors $\vec{\mu}$ indicate linear combinations of misalignment angle $\vec{\alpha}$ and decenter $\vec{\ell}$.

In Table 2 we give only the dependence upon pupil position and field angle for the symmetric fifth-order aberration patterns and their associated misalignment patterns. For the third-order aberrations, there was one misalignment pattern each associated with coma,

astigmatism and curvature of field, with two misalignment patterns associated with distortion. There are again distinct σ and ρ misalignment patterns for fifth-order distortion, and now also for fifth-order astigmatism and fifth-order coma.

4.3. fifth-order aberration patterns and alignment

The amplitudes of aberrations patterns implicit in Table 2 provide, at least in principle, additional information for use in aligning telescopes. But in all cases there are similarities between the fifth-order misalignment aberration patterns and their third-order counterparts. The ability to distinguish between the two depends, for the first group described below, upon the sampling of the wavefront, and, for the second group, upon the sampling of the field.

4.3.1. *second coma*

The misalignment aberration pattern for second coma, shown in Figure 8 is identical to that for ordinary (first) coma (see Figure 1). The point spread functions for second coma and ordinary (first) coma have the same azimuthal dependence on pupil position but different radial dependence. The ability to distinguish between the coma-II misalignment pattern and the coma-I misalignment pattern therefore depends critically upon the sampling of the wavefront.

4.3.2. *second astigmatism*

As with second coma, the aberration pattern for second astigmatism, shown in Figure 9 is identical to that for ordinary (first) astigmatism (see Figure 2). The point spread functions for second astigmatism and ordinary (first) astigmatism have the same angular dependence on pupil position but different radial dependence. The ability to distinguish between the astigmatism-II misalignment pattern and the astigmatism-I misalignment pattern again depends critically upon the sampling of the wavefront.

4.3.3. *fifth-order spherical*

The aberration patterns for fifth-order spherical, shown in Figure 10 are identical to those for those of curvature of field. The point spread functions for fifth-order spherical

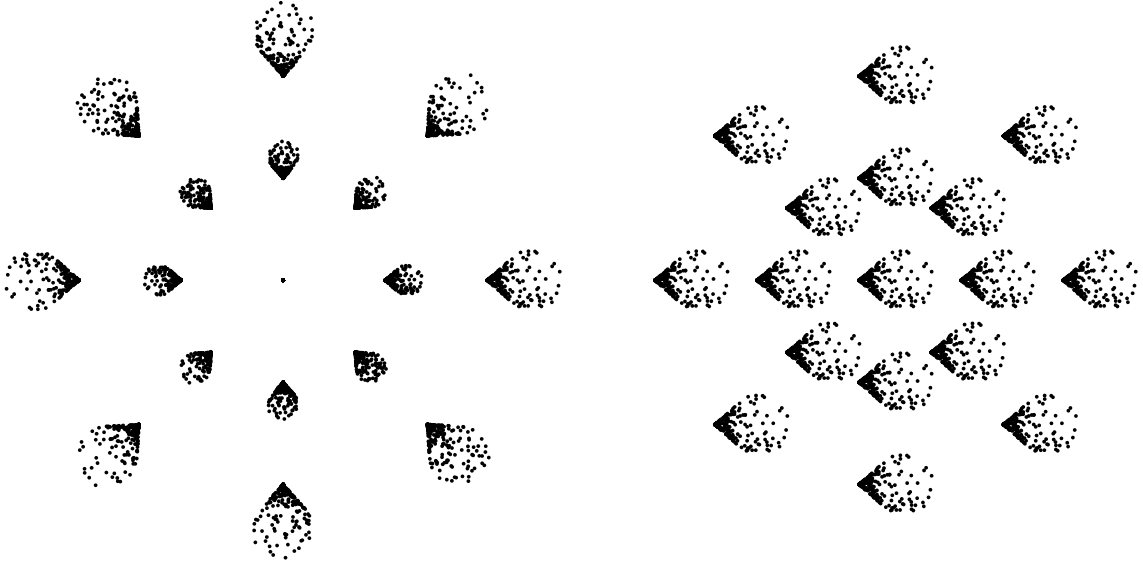


Fig. 8.— Second coma field patterns. (a) Second coma pattern typical of an aligned telescope. (b) Second coma pattern indicating a tilt and (or) decenter of a mirror along the x axis.

Table 2. Fifth-order aberration patterns

aberration	symmetric	misalignment
2nd spherical	$(\vec{\rho} \cdot \vec{\rho})(\vec{\rho} \cdot \vec{\rho})(\vec{\rho} \cdot \vec{\rho})$	
2nd coma	$(\vec{\rho} \cdot \vec{\rho})(\vec{\rho} \cdot \vec{\rho})(\vec{\rho} \cdot \vec{\sigma})$	$(\vec{\rho} \cdot \vec{\rho})(\vec{\rho} \cdot \vec{\rho})(\vec{\rho} \cdot \vec{\mu}_{cII})$
2nd astigmatism	$(\vec{\rho} \cdot \vec{\rho})(\vec{\rho} \cdot \vec{\sigma})(\vec{\rho} \cdot \vec{\sigma})$	$(\vec{\rho} \cdot \vec{\rho})(\vec{\rho} \cdot \vec{\sigma})(\vec{\rho} \cdot \vec{\mu}_{aII})$
fifth-order spherical	$(\vec{\rho} \cdot \vec{\rho})(\vec{\rho} \cdot \vec{\rho})(\vec{\sigma} \cdot \vec{\sigma})$	$(\vec{\rho} \cdot \vec{\rho})(\vec{\rho} \cdot \vec{\rho})(\vec{\sigma} \cdot \vec{\mu}_{5s})$
trefoil	$(\vec{\rho} \cdot \vec{\sigma})(\vec{\rho} \cdot \vec{\sigma})(\vec{\rho} \cdot \vec{\sigma})$	$(\vec{\rho} \cdot \vec{\sigma})(\vec{\rho} \cdot \vec{\sigma})(\vec{\rho} \cdot \vec{\mu}_t)$
fifth-order coma	$(\vec{\rho} \cdot \vec{\rho})(\vec{\rho} \cdot \vec{\sigma})(\vec{\sigma} \cdot \vec{\sigma})$	$(\vec{\rho} \cdot \vec{\rho})(\vec{\rho} \cdot \vec{\sigma})(\vec{\sigma} \cdot \vec{\mu}_{5c\sigma})$ $(\vec{\rho} \cdot \vec{\rho})(\vec{\sigma} \cdot \vec{\sigma})(\vec{\rho} \cdot \vec{\mu}_{5c\rho})$
fifth-order astigmatism	$(\vec{\rho} \cdot \vec{\sigma})(\vec{\rho} \cdot \vec{\sigma})(\vec{\sigma} \cdot \vec{\sigma})$	$(\vec{\rho} \cdot \vec{\sigma})(\vec{\rho} \cdot \vec{\sigma})(\vec{\sigma} \cdot \vec{\mu}_{5a\sigma})$ $(\vec{\rho} \cdot \vec{\sigma})(\vec{\sigma} \cdot \vec{\sigma})(\vec{\rho} \cdot \vec{\mu}_{5a\rho})$
fifth-order defocus	$(\vec{\rho} \cdot \vec{\rho})(\vec{\sigma} \cdot \vec{\sigma})(\vec{\sigma} \cdot \vec{\sigma})$	$(\vec{\rho} \cdot \vec{\rho})(\vec{\sigma} \cdot \vec{\sigma})(\vec{\sigma} \cdot \vec{\mu}_{5f})$
fifth-order distortion	$(\vec{\rho} \cdot \vec{\sigma})(\vec{\sigma} \cdot \vec{\sigma})(\vec{\sigma} \cdot \vec{\sigma})$	$(\vec{\rho} \cdot \vec{\sigma})(\vec{\sigma} \cdot \vec{\sigma})(\vec{\sigma} \cdot \vec{\mu}_{5d\sigma})$ $(\vec{\sigma} \cdot \vec{\sigma})(\vec{\sigma} \cdot \vec{\sigma})(\vec{\rho} \cdot \vec{\mu}_{5d\rho})$

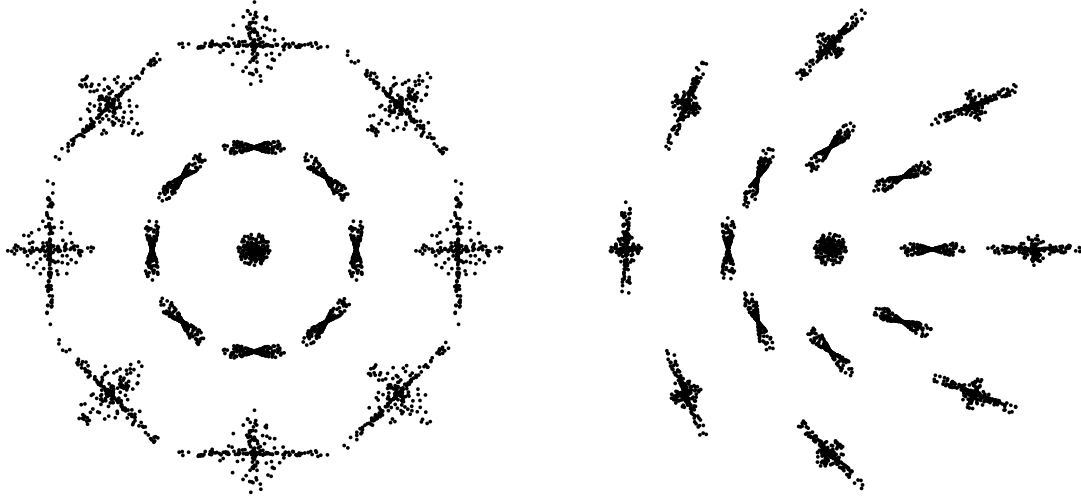


Fig. 9.— Second astigmatism field patterns. (a) Second astigmatism patterns typical of an aligned telescope. (b) Second astigmatism pattern indicating a tilt and (or) decentering of a mirror along the x axis.

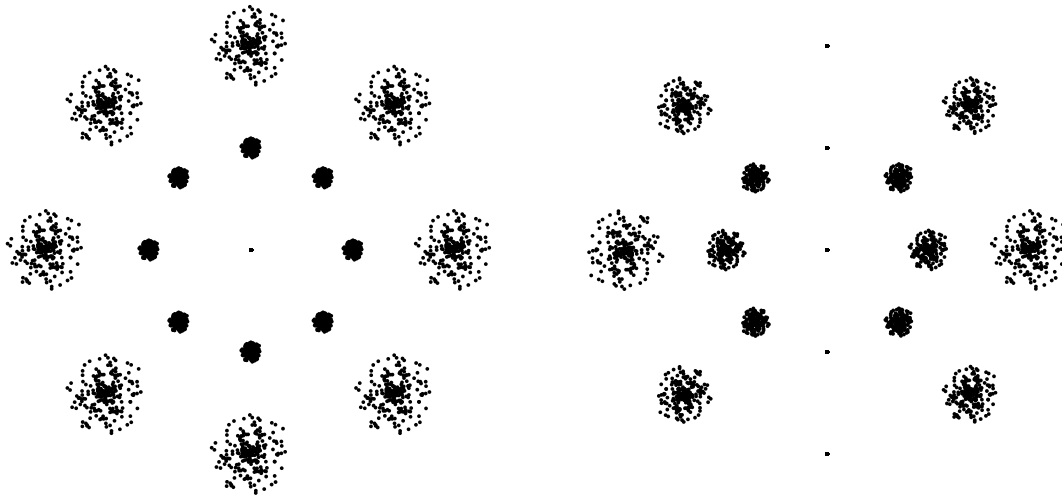


Fig. 10.— Fifth-order spherical field patterns. (a) Spherical aberration pattern typical of an aligned telescope. (b) Spherical aberration indicating a tilt and (or) decenter of a mirror along the x axis.

and defocus have the same angular dependence on pupil position but different radial dependence. The ability to distinguish between the fifth-order spherical and curvature of field misalignment pattern once again depends critically upon the sampling of the wavefront.

4.3.4. *trefoil*

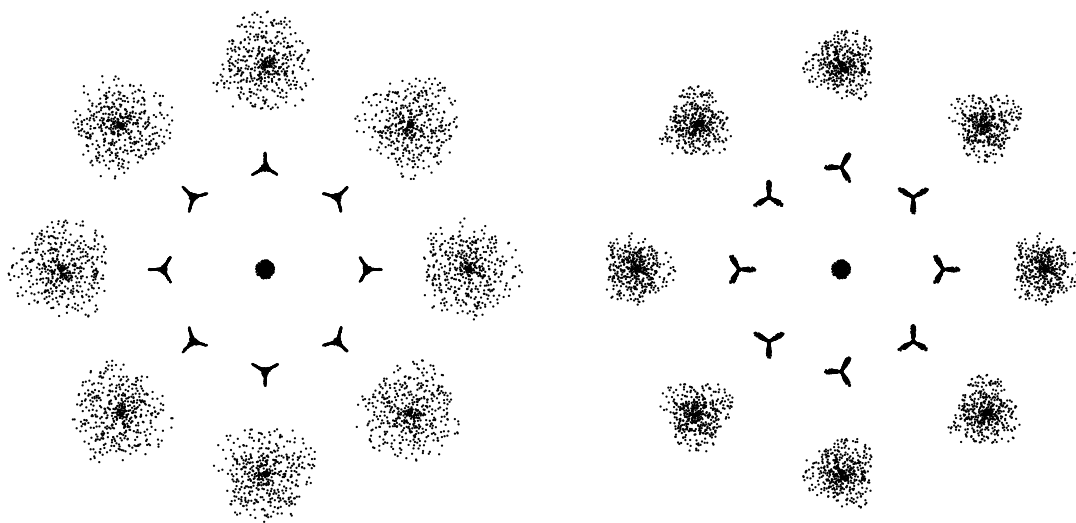


Fig. 11.— Trefoil field patterns. (a) Trefoil pattern characteristic of an aligned telescope. (b) Trefoil indicating a tilt and (or) decenter of a mirror along the x axis. In both cases a constant wavefront varying as ρ^3 has been added to bring out the orientation of the aberration.

The PSF for trefoil is quite different from that of any of the Seidel third-order aberrations, as is its misalignment pattern, shown in Figure 11.

4.3.5. *fifth-order astigmatism*

The PSF for fifth-order astigmatism is identical to that of Seidel, third-order astigmatism. But the two misalignment aberration patterns shown in Figure 12 are unlike third-order misalignment astigmatism (see Figure 2). The ρ misalignment pattern has the same azimuthal field dependence as for third-order astigmatism, but has a different radial dependence. The σ misalignment pattern has a different azimuthal field dependence and a different radial dependence. The ability to distinguish between the two fifth-order astigmatism mis-

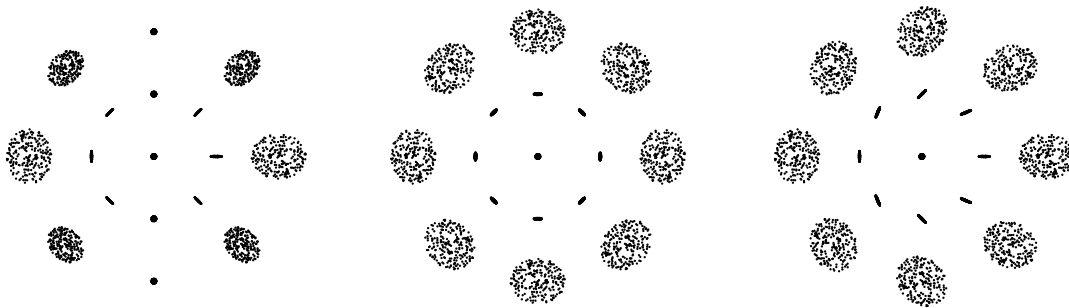


Fig. 12.— Fifth-order astigmatism field patterns. (a) The “ σ ” astigmatism pattern indicating a tilt and (or) decentering of a mirror along the x axis. Note that the astigmatism is radially aligned. (b) Astigmatism pattern typical of an aligned telescope. (c) The “ ρ ” astigmatism pattern indicating a tilt and (or) decentering of a mirror along the x axis. Note that the azimuthal dependence on field angle is identical to that for third-order misalignment astigmatism. A constant defocus has been added to all three panels to show the orientations of the aberrations.

alignment patterns and the third-order astigmatism misalignment pattern therefore depends critically upon the sampling of the field rather than the wavefront.

4.3.6. *fifth-order coma*

As with fifth-order astigmatism, the PSF for fifth-order coma is identical to that of Seidel, third-order coma. But the two misalignment aberration patterns shown in Figure 13 are unlike third-order misalignment coma (see Figure 1). The ρ misalignment pattern has the same azimuthal field dependence as for third-order coma, but different radial dependence. The σ misalignment pattern has a different azimuthal field dependence and a different radial dependence. As with fifth-order astigmatism, the ability to distinguish between the two fifth-order coma misalignment patterns and the third-order coma misalignment pattern therefore depends critically upon the sampling of the field rather than the wavefront.

4.3.7. *fifth-order defocus*

As with fifth-order astigmatism and coma, the PSF for fifth-order defocus is identical to that of curvature of field (which might equally well be called third-order defocus). But the

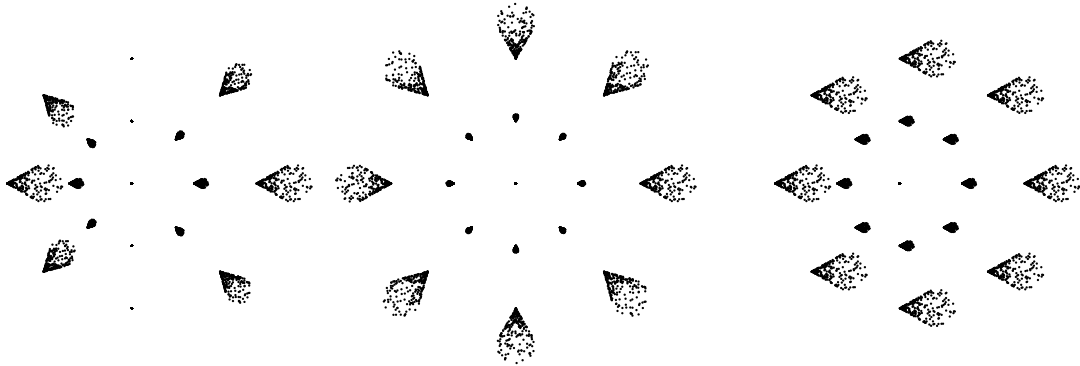


Fig. 13.— Fifth-order coma field patterns. (a) The “ σ ” coma pattern indicating a tilt and (or) decentering of a mirror along the x axis. Note that the coma is radially aligned. (b) Coma characteristic of an aligned telescope (c) The “ ρ ” coma pattern indicating a tilt and (or) decentering of a mirror along the x axis. Note that the azimuthal dependence on field angle is identical to that for third-order misalignment coma.

misalignment aberration patterns are not identical. They have same angular dependence, but exhibit a different radial dependence. Once again, the ability to distinguish between the fifth-order defocus misalignment pattern and the curvature of field misalignment pattern depends critically upon the sampling of the field rather than the wavefront.

4.4. discussion of fifth-order misalignment aberration patterns

The literature on fifth-order aberrations is limited for several reasons. First, by their very nature, they tend to be smaller than the third-order (Seidel) aberrations. Second, they are rather cumbersome. As a matter of course, ray tracing programs handle them correctly, so as a matter of practice, they receive little attention.

But as we have seen in the previous section, fifth-order aberrations may be needed to keep a three-mirror telescope aligned, and would almost certainly be needed to keep a four-mirror telescope aligned. Conversely, if one uses only third-order aberrations to keep a telescope aligned, there are degenerate telescope configurations that zero out the third-order misalignment aberrations and yet produce fifth-order misalignment aberrations. It is therefore of some interest to estimate which of these might be more or less substantial.

An order of magnitude argument can be made by noting that the entries in Table 2 are homogeneous and of sixth order in the sum of the exponents of the pupil radius and the field angle. Both of these are rendered dimensionless by the focal lengths. We would argue that

it is the focal ratio of the fastest element that matters most in such considerations. Modern fast, wide field telescopes have primary f-ratios approaching unity, while the field angles are rarely greater than a tenth of a radian. By this argument the terms at the top of Table 2 would be larger than those at the bottom.

But as we have seen above, the accuracy with which one can distinguish between fifth-order misalignment aberration patterns and their associated third-order patterns depends upon how finely one samples the point spread function and the field. Sampling the wavefront more finely requires brighter (and therefore rarer) stars. And allowing additional degrees of freedom in fitting the wavefront renders all of the measurements more uncertain. But sampling the field more finely requires more wavefront sensors, which means less of the field is available for science.

4.5. Tessieres models for the LSST

The approach advocated here is quite similar to that adopted by Regis Tessieres in an unpublished M.S. thesis (2003) carried out at the University of Arizona. Tessieres analyzed the off-axis aberrations for two telescopes in terms of patterns derived in Thompson’s unpublished (1980) PhD thesis. But instead of computing the amplitudes of the patterns according to the principles set forth by Thompson, he used ray-tracing software to produce wavefronts across the field for various misalignments. He then fit these wavefronts to the expected patterns.

Of particular relevance for the present work, he analyzed an early version of the Large Synoptic Survey Telescope (Seppala 2002; henceforth LSST) in which the tertiary and primary were independent (rather than fabricated from a single monolith, as with the ultimate design). He applied decenters and tilts to the secondary and tertiary (and to the corrector assembly) and decomposed the computed wavefronts into the third- and fifth-order aberration patterns. Results of those calculations are given in Table 3, which shows the effects of tilts in the secondary and tertiary.⁶ Each entry gives the amplitude of the aberration at the edge of the field and at the edge of the pupil, in microns, for one degree of tilt. Up to factors of order unity the rms spot size will be proportional to these.

The first impression one gets is that the third-order aberrations are factors of 30-300 larger than the fifth-order aberrations. A consequence of this disparity is that, to the extent

⁶Tessieres’ nomenclature is similar to Hopkins’, but each aberration is preceded by its field angle dependence. Thus what we would call third-order misalignment astigmatism he calls field-linear astigmatism.

that the fifth-order and third-order aberration patterns are correlated, a small relative error in a measurement of a third-order aberration pattern will produce a large relative error in the corresponding fifth-order aberration pattern. This bodes ill for using fifth-order aberrations for telescope alignment. Tessieres’ calculations are themselves not entirely immune from such errors, but Tessieres had the luxury of measuring the wavefront with high precision at a large number of points in the field.

There are several patterns for which Tessieres did not report amplitudes – fifth-order astigmatism- σ and the ρ patterns for fifth-order coma and astigmatism for the secondary mirror. One suspects that the amplitudes for these were so small as to be in the noise, but Tessieres is not explicit on this point.

Tessieres *did* fit several patterns that vary quadratically with tilt and decenter. We suspect that the coefficients for these would approach zero for successively smaller tilts and decenters. Assuming iterative alignment correction these will play no role once the misalignments are small, and we have not included them in our discussion.

Tessieres did not measure the misalignment patterns for either spherical aberration or curvature of field (defocus). These surely contributed to his figure of merit, and his alignment experiments might have converged more rapidly had he measured them.

Finally Tessieres did not measure distortion, which might in principle be used to align a telescope if there is sufficiently accurate pre-existing astrometry.

4.6. Manuel’s models for the HET corrector

In another unpublished Ph.D. thesis, Anastacia Manuel (2009), working at the University of Arizona, carried out a ray-tracing a misalignment analysis of a four-element corrector for the Hobby-Eberly telescope.

The emphasis was on identifying the combinations of motions of the four elements that produced the largest aberrations using singular value decomposition. These modes sometimes involved more than one of the modes considered here. Several of the larger modes were associated with despacing and manifested themselves in symmetric aberration patterns.

But of the misalignment patterns, the three largest were the misalignments associated coma, curvature of field, and astigmatism, all of which are third-order. Next after that came linear combinations of second coma and second astigmatism misalignment patterns. These modes produced a figure of merit (which we take to be proportional to the wavefront error) a factor of 10^4 smaller than those for coma-I and a factor of 30 smaller than those for

Table 3. Amplitude of misalignment patterns at edge of the field for an early version of the LSST, in microns for tilts of 1 deg.

here	Tessieres	M2	M3
third-order coma	constant coma	178	186
third-order astigmatism	linear astigmatism	114	36
coma-II	constant fifth-order coma	2.4	4.3
astigmatism-II	linear oblique spherical	0.58	0.17
trefoil	quadratic elliptical coma	0.41	0.49
fifth-order coma- σ	quadratic coma#2	0.90	2.09
fifth-order coma- ρ	quadratic coma#1	^a	3.5
fifth-order astigmatism- ρ	cubic astigmatism#1	^a	1.72

^ano value given

astigmatism-I. This would again suggest that measurements of fifth-order aberrations may not contribute much to aligning the system in question.

5. Complications

5.1. mirror deformation

We have until now treated the mirrors of a telescope as rigid bodies. But under the influence of changing gravitational and thermal stresses, the mirror surfaces deform and influence the wavefront. Deformations of the mirrors can be expanded in terms of Zernike polynomials, but it is more efficient to expand them in terms of their elastic bending modes (Noethe 1991; Martin et al. 1998; Schechter et al. 2003).

If the stop is coincident with one of the mirrors, then the deformations of that mirror have the same effect on the wavefront at every point in the field. But if not, deformations of a mirror will project onto different parts of the pupil at different points in the field. Distinguishing deformations of two or more different mirrors therefore requires good sampling of the wavefront.

Among the fifth-order aberrations, second-coma, second-astigmatism and fifth-order spherical likewise require good sampling of the pupil to distinguish their misalignment patterns from those of third order aberrations. The accuracy with which one might determine these fifth-order aberrations is diminished by the need to use the same information to determine the mirror deformations.

This would argue for using two kinds of wavefront sensors: low-order sensors, using only coma, astigmatism and defocus to correct the rigid body motions, and high-order sensors to correct for mirror deformations. The latter might be run at lower cadence than the former, except perhaps immediately following a large change in telescope pointing.

In such a scheme one might still measure fifth-order misalignment coma and fifth-order misalignment astigmatism with the low-order wavefront sensors, but one would need a sufficient number of field samples to discriminate between the third- and fifth-order aberration patterns. Merely sampling on the periphery will not permit discrimination between fifth-order misalignment astigmatism- ρ and third-order misalignment astigmatism. The same holds true for fifth-order misalignment coma- ρ and third-order misalignment astigmatism. If the telescope is then properly aligned the second-coma and second-astigmatism misalignment patterns will be zeroed out on the high-order wavefront sensors, giving a cleaner measurement of the mirror deformations.

5.2. central obscuration

Many wide field telescope designs have a large central obscuration. This would make it more difficult to distinguish between second coma and second astigmatism on the one hand and ordinary coma and astigmatism on the other, which in third-order have the same field pattern. The smaller range of pupil radii would increase correlated errors.

5.3. degeneracies

As we have noted, the third-order misalignment patterns measured by wavefront sensors can correct a 2.5-mirror telescope. A 3-mirror telescope that uses only these patterns will have two uncontrolled degrees of freedom, and will in general produce third-order misalignment distortion and all of the fifth-order misalignment aberration patterns. Moreover these will vary with time.

For some purposes these might prove relatively benign. Distortion does not affect the point spread function and fifth-order misalignment aberrations tend to be small. But a random walk through the uncontrolled degrees of freedom will eventually produce large fifth-order misalignment aberrations and may also produce third-order misalignment patterns that are second order in tilts and decenters.

Metrology might suffice to keep the otherwise degenerate tilts and decenters small enough that the fifth-order aberrations do not present a problem. Alternatively, tilts and decenters might be corrected by measuring distortion misalignment patterns. The pre-existing astrometry may not need to be very accurate if the goal is only to keep the fifth-order aberrations in check. For fast telescopes one might consider using galaxies rather than stars to minimize the effects of proper motions. But the distortion signal may itself be weak since the pattern varies as a higher power of field angle than astigmatism or coma.

5.4. pointing

In the same way that spherical aberration might equally well have been called “second defocus” – the two have same dependence upon pupil azimuth – distortion might equally well have been called “second tilt.” Tilt is one of only two first-order aberrations and cannot be measured with a wavefront sensor. In a paper on the Advanced Solar Telescope, Manuel & Burge (2009) suggest that one might use pointing to constrain telescope alignment. This would require accurate measurement of the position of the detector with respect to one

of the mirrors.

5.5. focal plane tilt

We have until this point avoided the question of how one knows the position of one’s wavefront sensors with respect to one or another of a telescope’s mirrors. As in the discussion of pointing in the previous subsection, this might be determined by precision measurement. But if not, and if one wishes to correct for focal plane tilt, one must add one additional aberration pattern. The misalignment curvature of field pattern is exactly what one expects from a tilted detector, but if it is used to correct the detector tilt it cannot also be used to keep the mirrors aligned.

5.6. transmitting correctors

In his treatment of the LSST, Tessieres (2003) studies the effects of tilts and decenters on a focal plane assembly consisting of a multi-element corrector and the focal plane array. Two additional patterns are needed to keep this assembly aligned. Interestingly, the fifth-order aberration patterns produced by these tilts and decenters are larger, compared to the third-order aberration patterns, than for the secondary and tertiary mirrors.

6. Using and not using misalignment aberration patterns

At least three of the generic misalignment aberration patterns described in the previous sections are currently used to align wide-field telescopes, and there may soon be reason to use more of them. Ignoring for the present, the question of whether or not to use distortion⁷ we imagine here an N -mirror telescope with n wavefront sensors distributed throughout the field each capable of measuring m aberrations. One must determine $N - 1$ tilts and $N - 1$ decenters, each of which is described by a two-vector.

⁷We take the view what can be measured can hurt you.

6.1. independent analysis of the wavefront sensors

The most straightforward and transparent approach is to analyze each wavefront sensor separately, determining the coefficients of the aberrations at each of m points in the field. One then fits these coefficients to a linear combination of the misalignment aberration patterns described in the previous section and finally fits the amplitudes of the misalignment patterns (assuming one has measured more patterns than one actually needs).⁸

A complication of this approach is that at each step the quantities for which one is fitting may be correlated with each other. Aberration coefficients will be correlated, pattern amplitudes will be correlated and tilts and decenters will be correlated. Under such circumstances one must be careful to fit for all correlated quantities; otherwise one runs the risk of introducing systematic errors in the quantities for which one does fit.

6.2. simultaneous fit of all wavefront sensors for pattern amplitudes

Instead of measuring the aberrations at each point in the field, one might fit the data for all n wavefront sensors simultaneously to determine the amplitudes of the misalignment aberration patterns. This has the advantage of eliminating the problem of correlated aberrations at each point, but unmodelled aberrations may then lead to systematic errors.

6.3. simultaneous fit of all wavefront sensors for tilts and decenters

One might also fit directly for the tilts and decenters, short-circuiting the misalignment aberration patterns except for using them to turn tilts and decenters into predicted wavefronts that are then compared with observed wavefronts. This reduces the number of parameters for which one fits and implicitly accounts for the correlations of aberration pattern amplitudes. Rather than fitting for poorly determined amplitudes of fifth-order aberration patterns, all of the fifth-order dependence is attributed to a smaller number of tilts and decenters, which are strongly constrained by the third-order aberration patterns.

⁸It would not be surprising if two or more patterns were produced by the same, or nearly the same combination of tilts and decenters.

6.4. forget about misalignment patterns

Finally one might dispense entirely with the decomposition of the wavefront into specific aberrations and instead use ray tracing to determine how it varies at each measured point. While this obviates the need for misalignment patterns, it sacrifices all understanding of why one might need n wavefront sensors with enough resolution to measure m aberrations.

7. Summary

We have derived and illustrated the generic third-order aberration patterns that arise when the axial symmetry of a telescope is broken by small misalignments of optical elements. There are five patterns: one each for coma, astigmatism and curvature of field and two for distortion. Each of these misalignment patterns is characterized by an associated two-dimensional vector. These two-vectors are in turn linear combinations of the tilt and decenter vectors of the individual optical elements.

For an N -mirror telescope, $2(N - 1)$ patterns must be measured to keep the telescope aligned. For $N = 3$, as in a three mirror anastigmat, there is a two-dimensional “subspace of benign misalignment” over which the misalignment patterns for third-order coma, astigmatism and curvature of field are identically zero. If pre-existing astrometry is available, one or both of the distortion patterns may be used to keep the telescope aligned. Alternatively, one might measure one of the fifth-order misalignment patterns.

We have illustrated the generic fifth-order misalignment patterns that arise from small misalignments. These are relatively insensitive to misalignments and may be of little use in telescope alignment. One would appear to be driven back to using distortion, or alternatively, pointing.

Acknowledgements: We gratefully acknowledge helpful and thought provoking conversations and communications with Michael Jarvis, Don Phillion, Lothar Noethe, Stephen Shectman and Tony Tyson.

A. Coma

Schroeder (1987), calculates the the coma pattern cause by tilting and decentering the secondary of a two mirror telescope by amounts α and ℓ .

$$\begin{aligned}
 G &= B_2 \rho^3 \sin \phi & (A1) \\
 B_2 &= B_2(cen) + \frac{1}{R_2^2} \left[\frac{l}{R_2} \left[K_2 - \left(\frac{m_2 + 1}{m_2 - 1} \right) \right] - \alpha \left(\frac{m_2 + 1}{m_2 - 1} \right) \right] \\
 B_2(cen) &= \frac{\theta}{R_1^2} - \frac{W\theta}{R_2^2} \left[\left(\frac{m_2 + 1}{m_2 - 1} \right) \left(\frac{1}{W} - \frac{1}{R_2} \right) + \frac{K_2}{R_2} \right]
 \end{aligned}$$

where ρ and ϕ are the radial and angular coordinates on the pupil and θ is the radial coordinate of the image in the field. The quantities R_i , K_i and m_i are all mirror properties: the radius of curvature, conic constant, and magnification of a mirror, where the subscript denotes which mirror is being addressed. Finally, W is the distance from the primary mirror to the secondary.

$B_2(cen)$ is the coma of an aligned two mirror telescope. For the sake of simplicity the tilt and decenter of the secondary from the primary, and the object displacement from the optical axis have been taken lie along the y axis in Schroeder's analysis.

Schroeder's equations can be generalized for an object displaced from the optical axis in an arbitrary direction. The chief ray for the object is given by $\vec{\sigma}$ with radial and angular components σ and θ . The equations can be further generalized to allow decentering and tilting of the secondary mirror in arbitrary directions $\vec{\ell}$ and $\vec{\alpha}$ with radial components ℓ and α and angular components ϕ_ℓ and ϕ_α . The equations become:

$$G = B_{2x} \rho^3 \cos \phi + B_{2y} \rho^3 \sin \phi \quad (A2)$$

where the field dependences are given by

$$\begin{aligned}
 B_{2x} &= G_{Seidel}^{coma} \sigma \cos \theta + G_{decenter}^{coma} \ell \cos \phi_\ell + G_{tilt}^{coma} \alpha \cos \phi_\alpha & (A3) \\
 B_{2y} &= G_{Seidel}^{coma} \sigma \sin \theta + G_{decenter}^{coma} \ell \sin \phi_\ell + G_{tilt}^{coma} \alpha \sin \phi_\alpha \\
 G_{Seidel}^{coma} &= \frac{1}{R_1^2} - \frac{W}{R_2^2} \left[\left(\frac{m_2 + 1}{m_2 - 1} \right) \left(\frac{1}{W} - \frac{1}{R_2} \right) + \frac{K_2}{R_2} \right] \\
 G_{decenter}^{coma} &= \frac{1}{R_2^3} \left[K_2 - \left(\frac{m + 1}{m - 1} \right) \right] \\
 G_{tilt}^{coma} &= -\frac{1}{R_2^3} \left(\frac{m + 1}{m - 1} \right)
 \end{aligned}$$

Consolidating the above equations yields

$$G^{coma} = G_{decenter}^{coma} \sigma \rho^3 \cos(\phi - \theta) + G_{decenter}^{coma} \ell \rho^3 \cos(\phi - \phi_\ell) + G_{tilt}^{coma} \alpha \rho^3 \cos(\phi - \phi_\alpha) \quad (A4)$$

which is the form for the coma aberration given in §2

B. Astigmatism

McLeod (1996) follows the notation of Schroeder and calculates the astigmatism pattern for a two mirror telescope for which the secondary mirror has been aligned (decentered) to null the field constant coma pattern. McLeod gives the form of the remaining astigmatism patterns as

$$\begin{aligned} W &= Z_4 \rho^2 \cos 2\phi + Z_5 \rho^2 \sin 2\phi & (B1) \\ Z_4 &= B_0(\theta_x^2 - \theta_y^2) + B_1(\theta_x \alpha_x - \theta_y \alpha_y) + B_2(\alpha_x^2 - \alpha_y^2) \\ Z_5 &= 2B_0(\theta_x \theta_y) + B_1(\theta_x \alpha_y + \theta_y \alpha_x) + 2B_2(\alpha_x \alpha_y) \\ B_0 &= A_0^p r_p^2 - A_0^s r_s^2 \\ B_1 &= -r_s^2 [2A_0^s + (W + d_n)A_1^s] \\ B_2 &= -r_s^2 [A_0^s + (W + d_n)A_1^s + (W + d_n)^2 A_2^s] \\ A_0 &= \frac{W^2}{2R} \left[\frac{K}{R^2} + \left(\frac{1}{W} - \frac{1}{R} \right)^2 \right] \\ A_1 &= \frac{W}{R^2} \left[\frac{1}{W} - \frac{K+1}{R} \right] \\ A_2 &= \frac{K+1}{2R^3} \end{aligned}$$

where ρ and ϕ are the (normalized) radial and angular coordinates on the pupil and θ_x and θ_y are the cartesian coordinates of the image in the field. The quantities R_i , K_i and m_i are again all mirror properties: the radius of curvature, conic constant, and magnification of a mirror, where the subscript denotes which mirror is being addressed, the primary p , or the secondary s . W is the distance from the primary mirror to the secondary, and α_x and α_y are the tilts of the secondary mirror with respect to the primary mirror.

McLeod additionally uses two constants which are not present in Schroeder's analysis of the coma pattern, r_i , which is the marginal ray height at the optic, and d_n , which denotes the

position of the coma free point. As McLeod nulled the misalignment coma prior to analyzing the astigmatism, the decenter of the system $\vec{\ell}$ is given by $\vec{\ell} = d_n \vec{\alpha}$. McLeod chose to express the astigmatism only in terms of the tilt of the secondary mirror, though he could have equivalently expressed the astigmatism only in terms of the decenter or as a combination of the two terms. For greater transparency of the field patterns caused by both decenters and tilts, we here decouple the decenter and tilt terms in McLeod's equations, removing the variable d_n . We also de-normalize the pupil coordinates and remove the terms which vary as the square of the misalignment.

$$\begin{aligned}
 W &= Z_4 \rho^2 \cos 2\phi + Z_5 \rho^2 \sin 2\phi & (B2) \\
 Z_4 &= B_0(\theta_x^2 - \theta_y^2) + B_{1decenter}(\theta_x \ell_x - \theta_y \ell_y) + B_{1tilt}(\theta_x \alpha_x - \theta_y \alpha_y) \\
 Z_5 &= 2B_0(\theta_x \theta_y) + B_{1decenter}(\theta_x \ell_y + \theta_y \ell_x) + B_{1tilt}(\theta_x \alpha_y + \theta_y \alpha_x) \\
 B_0 &= A_0^p r_p^2 - A_0^s r_s^2 \\
 B_{1decenter} &= 2A_0^s + W A_1^s \\
 B_{1tilt} &= A_1^s \\
 A_0 &= \frac{W^2}{2R} \left[\frac{K}{R^2} + \left(\frac{1}{W} - \frac{1}{R} \right)^2 \right] \\
 A_1 &= \frac{W}{R^2} \left[\frac{1}{W} - \frac{K+1}{R} \right]
 \end{aligned}$$

By converting the field variables to polar coordinates σ and ϕ_σ and similarly converting the misalignment variables to polar form ℓ , ϕ_ℓ , α , ϕ_α , the expression for the wavefront delay yields the form given in §2,

$$G^{astig} = G_{Seidel}^{astig} \sigma^2 \rho^2 \cos 2(\phi - \theta) + G_{decenter}^{astig} \sigma \ell \rho^2 \cos(2\phi - \theta - \phi_\ell) + G_{tilt}^{astig} \sigma \alpha \rho^2 \cos(2\phi - \theta - \phi_\alpha) \quad (B3)$$

where B_0 , $B_{1decenter}$ and B_{1tilt} are equal to G_{Seidel}^{astig} , $G_{decenter}^{astig}$ and G_{tilt}^{astig} .⁹

⁹The form of the astigmatism field pattern holds even for telescopes which have not been aligned to null the misalignment coma pattern. The expanded coefficients for the wavefront delay of a randomly misaligned telescope can be found in table 1.

C. Curvature of Field

The misalignment patterns for curvature of field are less well-explored in the literature. Thompson (2005) presents forms for the patterns, and we re-derive them here from the despaces and misalignments of a single mirror from the pupil.

As stated in §2.6, the contribution of a single mirror to the wavefront delay of the ray which strikes the mirror at position $\vec{\omega}$ and makes an angle $\vec{\psi}$ with the axis of the mirror is given by:

$$\begin{aligned} G^{3rd} = & W_{040} \left(\frac{\vec{\omega}}{R} \cdot \frac{\vec{\omega}}{R} \right) \left(\frac{\vec{\omega}}{R} \cdot \frac{\vec{\omega}}{R} \right) + W_{131} (\vec{\psi} \cdot \frac{\vec{\omega}}{R}) \left(\frac{\vec{\omega}}{R} \cdot \frac{\vec{\omega}}{R} \right) \\ & + W_{222} (\vec{\psi} \cdot \frac{\vec{\omega}}{R}) (\vec{\psi} \cdot \frac{\vec{\omega}}{R}) + W_{220} (\vec{\psi} \cdot \vec{\psi}) \left(\frac{\vec{\omega}}{R} \cdot \frac{\vec{\omega}}{R} \right) \\ & + W_{311} (\vec{\psi} \cdot \vec{\psi}) (\vec{\psi} \cdot \frac{\vec{\omega}}{R}) \end{aligned} \quad (C1)$$

where W_{040} is the spherical aberration coefficient, W_{131} is the coma coefficient, W_{222} is the astigmatism coefficient, W_{220} is the curvature of field coefficient, and W_{311} is the distortion coefficient. These aberration coefficients depend only on the curvature of the mirror, R , the conic constant of the mirror, K , the magnification of the mirror, m and the position of the object for the mirror, s .

The transformations from pupil coordinates $\vec{\rho}$ and $\vec{\sigma}$ to mirror coordinates for a mirror despaced by an amount W and decentered and tilted by \vec{l} and $\vec{\alpha}$ are

$$\vec{\psi} = \left(1 - \frac{W}{s} \right) \vec{\sigma} - \left(\vec{\alpha} + \frac{\vec{l}}{s} \right) \quad (C2)$$

$$\vec{\omega} = (\vec{\rho} - W\vec{\psi}) - \vec{l}. \quad (C3)$$

Expanding the wavefront delay caused by a single mirror in terms of the pupil coordinates and keeping only those terms which vary as ρ^2 on the pupil¹⁰ and vary linearly with the misalignments or less, we find an expression for the curvature of field wavefront delay added by a single offset mirror.

¹⁰The astigmatic component of the wavefront additionally has terms which vary as ρ^2 on the pupil. We exclude these astigmatic terms in the analysis of COF

$$\begin{aligned}
G_i^{COF} = & \left[\frac{1}{2} \left(\frac{W}{s} - 1 \right)^2 W_{220} + \frac{W}{R} \left(\frac{W}{s} - 1 \right) W_{131} + 2 \frac{W^2}{R^2} W_{040} \right] \left(\frac{\vec{\rho}}{R} \cdot \frac{\vec{\rho}}{R} \right) (\vec{\sigma} \cdot \vec{\sigma}) \quad (C4) \\
& + \left[2 \left(\frac{R}{s} \right) \left(\frac{W}{s} + 1 \right) W_{220} + \left(\frac{2W}{s} + 1 \right) W_{131} + 4 \frac{W}{R} W_{040} \right] \left(\frac{\vec{\rho}}{R} \cdot \frac{\vec{\rho}}{R} \right) \left(\vec{\sigma} \cdot \frac{\vec{l}}{R} \right) \\
& + \left[2 \left(\frac{W}{s} + 1 \right) W_{220} + \frac{W}{R} W_{131} \right] \left(\frac{\vec{\rho}}{R} \cdot \frac{\vec{\rho}}{R} \right) (\vec{\sigma} \cdot \vec{\alpha})
\end{aligned}$$

For a two mirror telescope, the primary and the secondary both contribute to the wavefront delay. As the primary is neither despaced nor misaligned from the pupil, the form of its contribution to the wavefront delay is simplified; notably, the primary mirror only contributes to the Seidel aberration. The secondary mirror is despaced and possibly misaligned from its pupil and therefore contributes to the decenter and tilt terms as well as the Seidel pattern. Combining the effects of the primary and secondary mirror yields:

$$\begin{aligned}
G^{COF} = & G_{Seidel}^{COF} (\vec{\sigma} \cdot \vec{\sigma}) (\vec{\rho} \cdot \vec{\rho}) + G_{decenter}^{COF} (\vec{\sigma} \cdot \vec{\ell}) (\vec{\rho} \cdot \vec{\rho}) + G_{tilt}^{COF} (\vec{\sigma} \cdot \vec{\alpha}) (\vec{\rho} \cdot \vec{\rho}) \quad (C5) \\
G_{Seidel}^{COF} = & R_1^2 W_{220_1} + R_2^2 \left[\frac{1}{2} \left(\frac{W}{s_2} - 1 \right)^2 W_{220_2} + \frac{W}{R_2} \left(\frac{W}{s_2} - 1 \right) W_{131_2} + 2 \frac{W^2}{R_2^2} W_{040_2} \right] \\
G_{decenter}^{COF} = & -R_2^3 \left[2 \left(\frac{R_2}{s_2} \right) \left(\frac{W}{s_2} + 1 \right) W_{220_2} + \left(\frac{2W}{s_2} + 1 \right) W_{131_2} + 4 \frac{W}{R_2} W_{040_2} \right] \\
G_{tilt}^{COF} = & -R_2^2 \left[2 \left(\frac{W}{s_2} + 1 \right) W_{220_2} + \frac{W}{R_2} W_{131_2} \right]
\end{aligned}$$

which is the form for the COF wavefront delay that appears in §2.

D. Distortion

The distortion field patterns can additionally be derived from the wavefront delay caused by a single optic. Again expanding equation (C1) in terms of pupil coordinates, but now retaining only those terms which vary as ρ on the pupil and vary linearly with the misalignments or less yields the expression for the distortion contribution of a single mirror which is despaced by W , decentered by $\vec{\ell}$ and tilted by $\vec{\alpha}$:¹¹

¹¹As noted in §2, we have omitted the W_{311} coefficient as it is equal to zero.

$$\begin{aligned}
G_i^{distortion} = & - \left[2 \frac{W}{R} \left(\frac{W}{s} - 1 \right)^2 (W_{220} + W_{222}) + 3 \frac{W^2}{R^2} \left(\frac{W}{s} - 1 \right) W_{131} + 4 \frac{W^3}{R^3} W_{040} \right] \left(\frac{\vec{\rho}}{R} \cdot \vec{\sigma} \right) (\vec{\sigma} \cdot \vec{\sigma}) \\
& (D1) \\
& - \left[4 \left(\frac{W}{s} \right) \left(\frac{W}{s} - 1 \right) W_{220} + 2 \left(\frac{W}{s} - 1 \right) \left(\frac{2W}{s} - 1 \right) W_{222} \right. \\
& \quad \left. + 4 \frac{W}{R} \left(\frac{3W}{2s} - 1 \right) W_{131} + 8 \frac{W^2}{R^2} W_{040} \right] \left(\frac{\vec{\rho}}{R} \cdot \vec{\sigma} \right) \left(\vec{\sigma} \cdot \frac{\vec{l}}{R} \right) \\
& - \left[2 \frac{W}{R} \left(\frac{W}{s} - 1 \right) (2W_{220} + W_{222}) + 2 \frac{W^2}{R^2} W_{131} \right] \left(\frac{\vec{\rho}}{R} \cdot \vec{\sigma} \right) (\vec{\sigma} \cdot \vec{\alpha}) \\
& - \left[2 \left(\frac{W}{s} - 1 \right)^2 W_{220} + 2 \left(\frac{W}{s} \right) \left(\frac{W}{s} - 1 \right) W_{222} \right. \\
& \quad \left. + 2 \frac{W}{R} \left(\frac{3W}{2s} - 1 \right) W_{131} + 4 \frac{W^2}{R^2} W_{040} \right] \left(\frac{\vec{\rho}}{R} \cdot \frac{\vec{l}}{R} \right) (\vec{\sigma} \cdot \vec{\sigma}) \\
& - \left[2 \frac{W}{R} \left(\frac{W}{s} - 1 \right) W_{222} + \frac{W^2}{R^2} W_{131} \right] \left(\frac{\vec{\rho}}{R} \cdot \vec{\alpha} \right) (\vec{\sigma} \cdot \vec{\sigma})
\end{aligned}$$

For a two mirror telescope, only the secondary contributes to the distortion wavefront delay, as the primary is by construct not despaced from its entrance pupil. Grouping the coefficients in the above equation into terms of field dependences yields the form for distortion in §2:

$$\begin{aligned}
G^{distortion} = & G_{Seidel}^{distortion} \sigma^3 \rho \cos(\phi - \theta) \\
& + G_{decenter,\sigma}^{distortion} \sigma^2 \ell \cos(\theta - \phi_\ell) \rho \cos(\phi - \theta) + G_{decenter,\rho}^{distortion} \sigma^2 \ell \rho \cos(\phi - \phi_\ell) \\
& + G_{tilt,\sigma}^{distortion} \sigma^2 \alpha \cos(\theta - \phi_\alpha) \rho \cos(\phi - \theta) + G_{tilt,\rho}^{distortion} \sigma^2 \alpha \rho \cos(\phi - \phi_\alpha)
\end{aligned} \tag{D2}$$

The coefficients are given by:

$$G_{Seidel}^{distortion} = \frac{1}{R} \left[2 \frac{W}{R} \left(\frac{W}{s} - 1 \right)^2 (W_{220} + W_{222}) + 3 \frac{W^2}{R^2} \left(\frac{W}{s} - 1 \right) W_{131} + 4 \frac{W^3}{R^3} W_{040} \right] \quad (D3)$$

$$G_{decenter,\sigma}^{distortion} = -\frac{1}{R^2} \left[4 \left(\frac{W}{s} \right) \left(\frac{W}{s} - 1 \right) W_{220} + 2 \left(\frac{W}{s} - 1 \right) \left(\frac{2W}{s} - 1 \right) W_{222} \right. \\ \left. + 4 \frac{W}{R} \left(\frac{3W}{2s} - 1 \right) W_{131} + 8 \frac{W^2}{R^2} W_{040} \right]$$

$$G_{decenter,\rho}^{distortion} = -\frac{1}{R^2} \left[2 \left(\frac{W}{s} - 1 \right)^2 W_{220} + 2 \left(\frac{W}{s} \right) \left(\frac{W}{s} - 1 \right) W_{222} \right. \\ \left. + 2 \frac{W}{R} \left(\frac{3W}{2s} - 1 \right) W_{131} + 4 \frac{W^2}{R^2} W_{040} \right]$$

$$G_{tilt,\sigma}^{distortion} = -\frac{1}{R} \left[2 \frac{W}{R} \left(\frac{W}{s} - 1 \right) (2W_{220} + W_{222}) + 2 \frac{W^2}{R^2} W_{131} \right]$$

$$G_{tilt,\rho}^{distortion} = -\frac{1}{R} \left[2 \frac{W}{R} \left(\frac{W}{s} - 1 \right) W_{222} + \frac{W^2}{R^2} W_{131} \right]$$

where all mirror properties and object distances refer to the secondary mirror, and the chief ray angle is the chief ray angle on the primary mirror.

REFERENCES

- Gitton, P., & Noethe, L. 1998, *The Messenger*, 92, 15
- Hopkins, H. H. 1950, Clarendon Press, Oxford.
- Hvisc, A. M., & Burge, J. H. 2008, *Proc. SPIE*, 7018,
- Lee, H., Dalton, G., Tosh, I.A.J., & Kim, S.-W. 2008, *Opt. Exp.*, 16, 10992.
- Ma, Z., Bernstein, G., Weinstein, A., & Sholl, M. 2008, *PASP*, 120, 1307
- Manuel, A. 2009, Ph.D. dissertation, University of Arizona, Tucson, Arizona.
- Manuel, A. M., & Burge, J. H. 2009, *Proc. SPIE*, 7433
- Maréchal, A., 1950, *Rev. Opt.*, 29, 1

- Martin, H. M., et al. 1998, Proc. SPIE, 3352, 412
- McLeod, B. A. 1996, PASP, 108, 217
- Noethe, L. 1991, J. Mod. Opt., Vol. 38, No. 6, p. 1043 - 1066, 38, 1043
- Noethe, L., & Guisard, S. 2000, Proc. SPIE, 4003, 382
- Palunas, P., et al. 2010, Proc. SPIE, 0, 0000
- Phillion, D. W., Olivier, S. S., Baker, K., Seppala, L., & Hvisc, S. 2006, Proc. SPIE, 6272
- Romano, A., et al. 2010, A&A, 514, A88
- Schechter, P. L., et al. 2003, Proc. SPIE, 4837, 619
- Schroeder, D. J. 1987, San Diego, CA, Academic Press, Inc, 363 p.
- Seppala, L. G. 2002, Proc. SPIE, 4836, 111
- Shack, R. V., & Thompson, K. 1980, Proc. SPIE, 251, 146
- Tessieres, R. 2003, M.S. thesis, University of Arizona, Tucson, Arizona.
- Thompson, K. 1980, Ph.D. dissertation, University of Arizona, Tucson, Arizona.
- Thompson, K. 2005, J. Opt. Soc. Am. A, 22, 1389
- Thompson, K., et al. 2009, J. Opt. Soc. Am. A, 26, 1503
- Wilson, R. N. 1996, Springer-Verlag Berlin Heidelberg New York, 543 p.
- Wilson, R. N., & Delabre, B. 1997, PASP, 109, 53
- Chandra X-ray Center 2009, The Chandra Proposer's Observatory Guide, Version 12. Retrieved from <http://cxc.harvard.edu/proposer/POG/>*